Ionic Liquid Confined in Nafion: Toward Molecular-Level Understanding

Delin Sun and Jian Zhou
School of Chemistry and Chemical Engineering, Guangdong Provincial Key Laboratory for Green Chemical Product Technology, South China University of Technology, Guangzhou 510640, P.R. China

DOI 10.1002/aic.14009
Published online February 19, 2013 in Wiley Online Library (wileyonlinelibrary.com)

In this article, multiscale simulation methods were used to study structural and transport properties of Nafion–ionic liquid composite membranes that are novel proton conducting materials for fuel cells. Coarse-grained model for 1-butyl-3-methylimidazolium tetrafluoroborate ([bmim][BF_4]) ionic liquid was first developed in the framework of BMW-MARTINI force field. Coarse-grained simulation results of bulk [bmim][BF_4] ionic liquid show good agreement with all-atom simulation results and experimental data. Nafion–[bmim][BF_4] composite membranes were then simulated using all-atom and coarse-grained models. Ionic liquid cluster formation inside Nafion was revealed by coarse-grained simulations. Diffusion coefficients of both $[bmim]^+$ cations and BF_4^- anions are reduced by one to two orders of magnitude depending on their concentrations in Nafion membrane. $[Bmim]^+$ cations have faster self-diffusion coefficient than BF_4^- anions, while this phenomenon is more pronounced when ionic liquids are confined in Nafion. This work provides molecular basis for understanding Nafion–ionic liquid composite membranes. © 2013 American Institute of Chemical Engineers
AIChE J, 59: 2630–2639, 2013
Keywords: fuel cell, Nafion, ionic liquid, molecular simulation, coarse-graining

Introduction

Nafion polymer is the state-of-the-art proton conducting material used for fuel cells. Proton conducting properties of conventional Nafion membrane strongly depend on the membrane's water content. To maintain high water content in Nafion, operating temperature of fuel cells cannot exceed 100°C, the boiling point of water under atmospheric pressure. Nonetheless, operation of proton exchange membrane fuel cells at elevated temperatures above 100°C is technically desirable, because it could both enhance reaction kinetics of electrodes and more importantly improve CO tolerance of the cost-prohibitive platinum catalyst.[1] In recent years, there are active research activities on the development of elevated-temperature proton conducting materials.[2–6] One promising approach is to replace water with ionic liquids at high temperatures.

Ionic liquids are versatile solvents that have low melting temperature, high ionic conductivity, excellent thermal and electrochemical stability, as well as negligible vapor pressure. These assorted merits of ionic liquids make them attractive to be incorporated into Nafion membrane to improve proton conductivity of the membrane at elevated temperatures and anhydrous conditions. Proton conducting properties of Nafion–ionic liquid composite membranes have been recently tested in experiments.[7–10] Experimental works demonstrate that Nafion/ionic liquid composite membranes not only possess improved proton conducting properties at high temperatures but also effectively mitigate the methanol crossover problem. These improved properties may be largely attributed to unique microstructures and transport properties of Nafion/ionic liquid composite membranes. Small-angle X-ray scattering, Fourier transform infrared spectroscopy, differential scanning calorimetry, and tapping mode atomic force microscopy experimental techniques have been increasingly utilized to understand the composite membranes[8,11–16]; nonetheless, molecular-level understanding of structural and transport properties of Nafion–ionic liquid composite membranes is still lacking. Molecular simulation methods including all-atom molecular dynamics[17–19] and coarse-grained modeling[20–23] have progressed as powerful tools to gain in-depth knowledge of Nafion membrane. Although virtually no reported molecular simulation work has concentrated on Nafion membrane impregnated with ionic liquids, this study primarily aims to understand structural and transport properties of Nafion/1-butyl-3-methylimidazolium tetrafluoroborate ([bmim][BF_4]) ionic liquid composite membrane utilizing coarse-grained and all-atom molecular dynamics (MD) simulation methods. We wish that this work could provide theoretical backgrounds for understanding and developing Nafion/ionic liquid composite membranes for elevated-temperature fuel cells.

Contract grant sponsor: New Century Excellent Talents in University; Contract grand number: NCET-07-0313.
Contract grant sponsor: National Natural Science Foundation of China; Contract grand numbers: 20706019; 20876052.
Contract grant sponsor: Guangdong Science Foundation; Contract grand number: S2011010002078.

Correspondence concerning this article should be addressed to J. Zhou at jianzhou@scut.edu.cn.

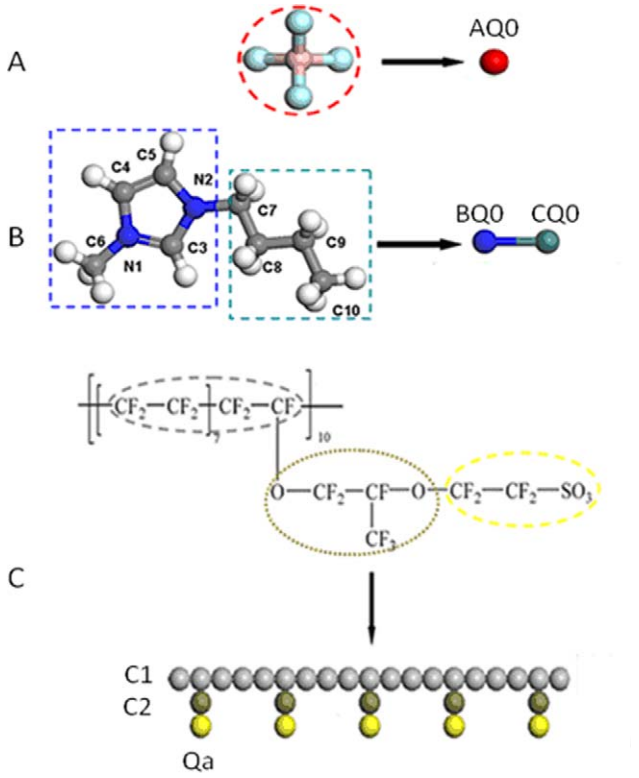

Scheme 1. All-atom and coarse-grained models of [bmim][BF_4] ionic liquid (a, b) and Nafion (c).

AQ0, BQ0, and CQ0 beads of ionic liquid and C1, C2, and Qa beads of Nafion are denoted by red, blue, cyan, gray, brown, and yellow colors, respectively. [Color figure can be viewed in the online issue, which is available at wileyonlinelibrary.com.]

Simulation Details

Coarse-grained model of [bmim][BF_4] ionic liquid

In this study, coarse-grained model of [bmim][BF_4] ionic liquid is developed in the framework BMW-MARTINI force field.[24,25] MARTINI is a generic coarse-grained force field initially developed for biomolecular simulations.[26] Recently, MARTINI has been successfully extended to study gold nanoparticles,[27] fullerenes,[28] and nanotubes,[29] as well as polymers.[20,30] To the best of our knowledge, no work has been reported to simulate ionic liquids using MARTINI force field. Developing a set of MARTINI compatible force field parameters for ionic liquids is highly significant to study issues including protein folding in ionic liquids, nanoparticle or polymer self-assembly in ionic liquids, ionic liquid diffusion in ionogels, mesoscopic morphologies of polyelectrolyte membranes, and so forth. These phenomena that normally require long simulation time were less reported using coarse-grained models largely due to the incompatibility of coarse-grained force field parameters. MARTINI force field may overcome this problem, yet the first challenging task is to develop reliable and MARTINI compatible coarse-grained models for ionic liquids.

The interaction potential of MARTINI force field is

$$U=4\varepsilon_{ij}\left[\left(\frac{\sigma_{ij}}{r}\right)^{12}-\left(\frac{\sigma_{ij}}{r}\right)^{6}\right]+\frac{q_i q_j}{4\pi\varepsilon_0\varepsilon_1 r} \quad (1)$$

It should be stressed herein that standard MARTINI force field utilizes a relative dielectric constant (ε_1) of 15 for screening electrostatic interactions,[26] and consequently standard MARTINI force field may be less accurate to describe interactions between charged species. Wu et al.[24] recently developed BMW-MARTINI model in which ε_1 is adjusted to 1.3. In this work, we report a set of BMW-MARTINI compatible parameters for [bmim][BF_4] ionic liquid. Simulating bulk [bmim][BF_4] ionic liquid in the framework of BMW-MARTINI force field, satisfying structural and dynamical results are obtained when compared with those of all-atom simulation results. These parameters are then used to study Nafion/[bmim][BF_4] composite membranes.

We use a simple three-site model to represent [bmim][BF_4] ionic liquid, as illustrated in Scheme 1a,b. One cation–anion pair is composed of three newly defined charged beads: AQ0, BQ0, CQ0, which respectively represent BF_4^- anion and two segments on $[bmim]^+$ cation. Bead charges are determined by summing atomic charges as defined in a united-atom model of [bmim][BF_4].[31] Considering the fact that both $[bmim]^+$ cation and BF_4^- anion are hydrophobic ions due to their chemical structures, the parameterization of Lennard-Jones (LJ) parameters for AQ0, BQ0, and CQ0 beads are mainly referred to apolar beads with low polarity in BMW-MARTINI force field. Detailed simulation parameters for [bmim][BF_4] are listed in Table 1.

In bulk ionic liquid simulations, all coarse-grained models contain 3000 cations and 3000 anions. After initial energy minimization, 100-ns coarse-grained MD simulations were performed in the isothermal–isobaric (NPT) ensemble, with the time step of 20 fs. The system's temperature was controlled with the Berendsen thermostat,[32] and the system's pressure was controlled with the Berendsen barostat at 1 bar with a compressibility value of 3.0×10^{-5} bar^{-1}. A cut-off of 1.2 nm was used for van der Waals (VDW) interactions, whereas electrostatic interactions with a relative dielectric constant of 1.3 were modeled using the particle-mesh Ewald summation method.[33] Both the energy and force vanish at the cut-off distance with the standard shift function of GROMACS 4.5.4 package.[34] To reduce the cut-off noise, the LJ potential was also smoothly shifted to zero from 0.9 to 1.2 nm. Bead coordinates were saved every 50 ps.

Table 1. Coarse-Grained Simulation Parameters for [bmim][BF_4] Ionic Liquid and Nafion Polymer

Bead Type	σ (nm)	ε (kJ·mol^{-1})	Charge
BQ0	0.47	3.5	0.6723
CQ0	0.47	3.5	0.3277
AQ0	0.47	3.5	−1
C1	0.47	3.5	0
C2	0.47	3.5	0
Qa	0.47	5.0	−1
Bond Type	**R_{bond} (nm)**	**K_{bond} (kJ mol^{-1} nm^{-2})**	
BQ0—CQ0	0.46	50,000	
C1—C1	0.43	1250	
C1—C2	0.43	1250	
C2—Qa	0.43	1250	
Angle Type	**θ_{angle} (°)**	**K_{angle} (kJ mol^{-1} rad^{-2})**	
C1—C1—C1	180	25	
C1—C1—C2	90	25	
C1—C2—Qa	180	25	

Table 2. Levels of LJ Interactions Among Different Bead Types[a]

	AQ0	BQ0	CQ0	C1	C2	Qa
AQ0	IV	V	IV	III	III	II
BQ0	V	IV	V	IV	IV	III
CQ0	IV	V	IV	III	III	II
C1	III	IV	III	IV	IV	III
C2	III	IV	III	IV	IV	III
Qa	II	III	II	III	III	I

[a]Level of LJ interactions according to BMW-MARTINI force field: I=attractive, ε=5.0 kJ mol^{-1}; II=almost attractive, ε=4.5 kJ mol^{-1}; III=semiattractive, ε=4.0 kJ mol^{-1}; IV=intermediate, ε=3.5 kJ mol^{-1}; V=almost intermediate, ε=3.1 kJ mol^{-1}.

Coarse-grained simulations of Nafion-[bmim][BF$_4$] membranes

Using MARTINI force field to simulate Nafion polymer was first reported by Malek et al.[20] In their study, one Nafion monomer contains only three beads. To comply with the nearly 4:1 mapping strategy of MARTINI force field, we use six beads to represent one Nafion monomer. The coarse-grained model of Nafion used in this work is illustrated in Scheme 1c. In each monomer, hydrophobic backbone is represented by four apolar C1 beads and side chain is represented by apolar C2 bead and charged Qa bead. Most simulation parameters including bond length and bond angle are referred to Malek et al.'s work.[20] Detailed simulation parameters for coarse-grained Nafion model are listed in Table 1. LJ parameters for different bead pairs are listed in Table 2. Starting configurations of composite membranes are built to mimic membranes fabricated using the two-step protocol,[7] that is, protonated Nafion membrane needs to be first neutralized with ionic liquid cations to exchange protons in the membrane; the neutralized Nafion membrane is then immersed into ionic liquid solution to swell. Each coarse-grained Nafion model consists of 50 repeating units and 50 such Nafion models are folded into a cubic simulation box with periodic boundary conditions on three dimensions. Microstructures of the composite membrane are studied by varying ionic liquid's concentration at λ=1.0, 1.5, and 2.0 (λ is defined as the ratio of the number of ionic liquid anion bead to the number of Qa bead on Nafion). The total number of cations thereby equal to the sum of Qa and AQ0 beads in the system. In our coarse-grained simulations, all beads are assumed to have the identical volume and mass. The corresponding weight fractions of ionic liquid in three composite membranes are 45, 52, and 57%, respectively. For each system, 300-ns coarse-grained MD simulations are run at different temperatures (300, 350, 373, 423, and 473 K) and 1 atm pressure. Most simulation parameters are the same as above except that simulation time step is reduced to 10 fs.

All-atom MD simulations

To validate our coarse-grained models of [bmim][BF$_4$] ionic liquid and Nafion–ionic liquid composite membrane, extensive all-atom MD simulations are also performed. The Nafion oligomer model consists of 10 monomers that are arranged in the dispersed sequence as described by Jang et al.'s work.[18] Starting configurations of all composite membrane models are generated using the PACKMOL package.[35] In each model, four Nafion polymer chains with all sulfonate groups in the protonated state are folded into a cubic simulation box with periodic boundary conditions in all directions. The number of cations and anions in the membrane is determined in the same way as coarse-grained simulations, that is, structural and transport properties of the ionic liquid are analyzed by varying ionic liquid's concentration in the membrane. Pristine [bmim][BF$_4$] ionic liquid containing 160 cation–anion pairs is also simulated.

In this study, a total of 120-ns MD simulation in the NPT ensemble was run to equilibrate each composite membrane model at three temperatures (373, 423, and 473 K). By monitoring density and total potential energy, it was found 20-ns MD simulations are sufficient to equilibrate the system. The last 100-ns trajectory files were thereby used for data analysis. For pristine ionic liquid, a total of 50-ns NPT-MD simulation was run at three temperatures, and the last 30-ns trajectory files were used for analysis. All-atom MD simulations were performed using the parallel version of LAMMPS (large-scale atomic/molecular massively parallel simulator) package from Plimpton at Sandia.[36] The velocity-Verlet algorithm[37] is used to integrate the equation of motion with a time step of 1.0 fs. The Nose–Hoover thermostat[38,39] and Andersen-Hoover[40] barostat with the damping relaxation time of 0.1 ps are, respectively, used to control temperature and pressure. The configurations are saved every 10 ps.

The refined Amber force field reparameterized by Liu et al.[41] is chosen to describe intramolecular and intermolecular interactions for [bmim][BF$_4$] ionic liquid. The generalized Amber force field (GAFF)[42] is used to simulate Nafion polymer. GAFF has the same functional form as Amber force field

$$E=\sum_{\text{bonds}} K_r(r-r_0)^2+\sum_{\text{angles}} K_\theta(\theta-\theta_0)^2 + \sum_{\text{dihedral}} \frac{K_\Phi}{2}[1+\cos(n\Phi-\gamma)]+\sum_{i<j}\left[\frac{A_{ij}}{r_{ij}^{12}}-\frac{B_{ij}}{r_{ij}^{6}}+\frac{q_iq_j}{r_{ij}}\right] \quad (2)$$

The four terms represent energies for bonds, angles, torsions, and nonbonded interactions including VDW and Coulombic interactions. Electrostatic and VDW interactions are calculated between atoms in different molecules or for atoms in the same molecule separated by at least three bonds. The nonbonded interactions separated by exactly three bonds are reduced by a scale factor, which is optimized as 0.5 for VDW and 0.8333 for electrostatic interactions. The LJ parameters for unlike atoms are obtained from the Lorentz–Berthelot combining rule. The cut-off radius is 1.0 nm for VDW interactions. Partial charges and force field parameters for Nafion polymer, [bmim]$^+$ cation, and BF_4^- cations are from Refs. 41 and 43. The particle–particle particle-mesh method[44] is used for electrostatic interactions.

Results and Discussion

Validation of coarse-grained model of [bmim][BF$_4$] ionic liquid

Both structural and dynamical properties are compared between coarse-grained and all-atom models to validate the accuracy of simplified coarse-grained model of [bmim][BF$_4$] ionic liquid used in this work.

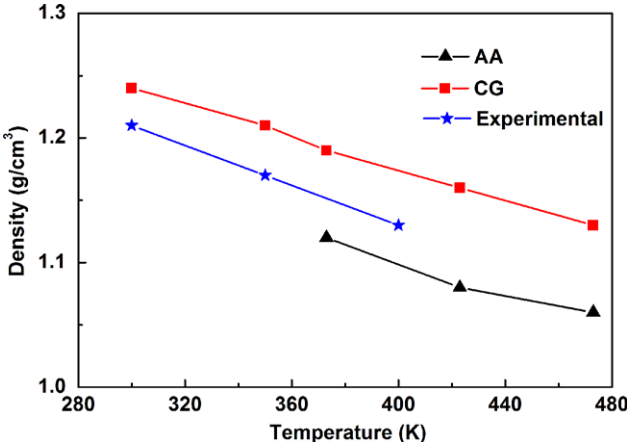

Figure 1. Comparison of simulated densities of [bmim][BF_4] ionic liquid with available experimental data.

[Color figure can be viewed in the online issue, which is available at wileyonlinelibrary.com.]

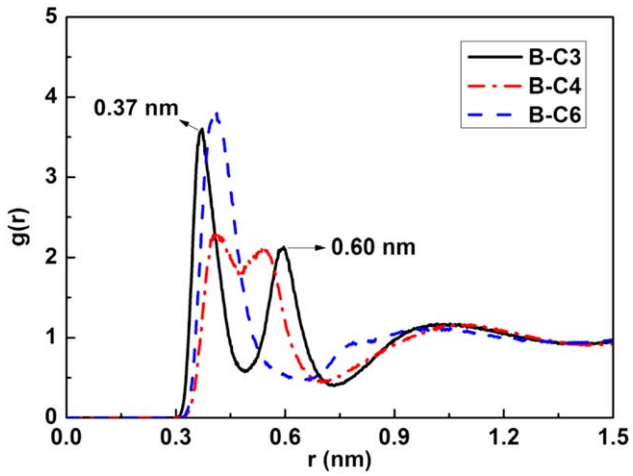

Figure 3. RDFs plotted between boron atom and C3, C4, and C6 atoms on cation.

[Color figure can be viewed in the online issue, which is available at wileyonlinelibrary.com.]

Densities

Figure 1 shows simulated densities of [bmim][BF_4] ionic liquid at varying temperatures. Results from both all-atom and coarse-grained simulation models are in agreements with available experimental data.

Radial distribution functions

The radial distribution function (RDF) indicates the probability density of finding A and B interacting sites at distance of r, averaged over the sampling trajectory

$$g_{A-B}(r) = \left(\frac{n_B}{4\pi r^2 dr}\right) \Big/ \left(\frac{N_B}{V}\right) \tag{3}$$

where n_B is the number of B particles located at the distance r in a shell of thickness dr from particle A; N_B is the number of B particles in the system; and V is the total volume of the system.

Figure 2a shows RDF curves plotted between AQ0-BQ0, AQ0-CQ0, and AQ0-AQ0 bead pairs from coarse-grained simulations. Figure 2b is RDF curves plotted between centers of mass of two segments on $[bmim]^+$ cation and center of mass of BF_4^- anion from all-atom simulations. Obviously, the coarse-grained model shows a higher and narrower RDF peak for cation–anion pair. This phenomenon was also reported in a recent four-site coarse-grained model of [bmim][BF_4] ionic liquid.[45] The reason for the curve shape disparity is analyzed in this study. Figure 3 shows RDF curves plotted between boron atom on anion and different carbon atoms on cation in all-atom model. For B—C3, B—C4 atom pairs, their RDF curves all show double peaks. This is in contrast to the sole peak appeared in the RDF curve for B—C6 atom pair. The double peaks arise from the structure of imidazolium ring. On the imidazolium ring, C3 and C4 atoms locate in directly opposite side. Each side of the imidazolium ring is likely to approach BF_4^-. In both configurations, the distance between C3 and B atoms are different; whereas the distance between C6 and B atoms are nearly equal. In the coarse-grained model, due to the absence of ring structure, only a single and high peak is observed. Actually, the RDF curve shape difference between coarse-grained and all-atom models is not surprising. As in the three-site coarse-grained model of ionic liquid, charges are more concentrated than in all-atom model. As anion mainly

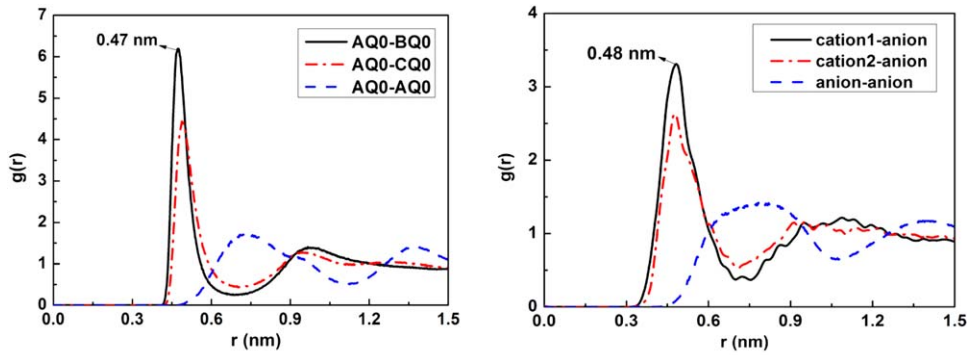

Figure 2. RDFs plotted between AQ0—BQ0, AQ0—CQ0, and AQ0—AQ0 bead pairs from coarse-grained model (a) and RDFs plotted between centers of mass of two segments on $[bmim]^+$ cation and center of mass of BF_4^- anion from all-atom model (b).

[Color figure can be viewed in the online issue, which is available at wileyonlinelibrary.com.]

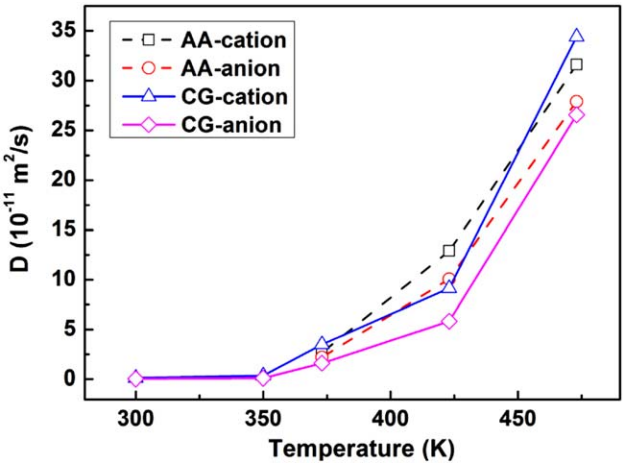

Figure 4. Self-diffusion coefficients of cations and anions computed from coarse-grained and all-atom simulations.

[Color figure can be viewed in the online issue, which is available at wileyonlinelibrary.com.]

interacts with C3 atom on the imidazolium ring in imidazolium-type ionic liquids,[46] the high peak centered at 0.47 nm in the RDF curve for BQ0—AQ0 bead pair can be viewed as the fusion of two peaks at 0.37 and 0.6 nm appeared in all-atom simulation results. This interpretation makes our three-site coarse-grained model capable of simulating key structural properties of [bmim][BF_4] ionic liquid.

Self-diffusion coefficients

Dynamical properties are compared between coarse-grained and all-atom models by analyzing self-diffusion coefficients of ionic liquid cations and anions. Self-diffusion coefficients of ionic liquid are calculated by the Einstein's relationship

$$D = \frac{1}{6N} \lim_{t\to\infty} \frac{d}{dt} \left\langle \sum_{i=1}^{N} [r_i(t) - r_i(0)]^2 \right\rangle \quad (4)$$

where N is the total number of cations or anions; $r_i(t)$ and $r_i(0)$ are the final and initial positions of mass center of cations or anions over the time interval t, respectively. The angle bracket represents the ensemble average of the mean-squared displacements (MSDs) of all cations or anions.

The computed self-diffusion coefficients of cations and anions at varying temperatures are plotted in Figure 4. The self-diffusion coefficients obtained from coarse-grained simulations show satisfying agreement with all-atom simulation results. Notably, the three-site coarse-grained model can reproduce the interesting phenomenon that larger-sized $[bmim]^+$ cations diffuse faster than smaller BF_4^- anions. This phenomenon was previously ascribed to the planar structure of imidazolium cations as well as the greater friction for translational motions of anions compared with cations.[47,48] While in our coarse-grained models, even in the absence of planar structure, cations can still diffuse faster than anions. The charge dispersion on larger-sized cation may be another possible explanation for this abnormal phenomenon.

In sum, the developed three-site coarse-grained model is able to reproduce key structural and dynamical properties of [bmim][BF_4] ionic liquid in a wide temperature range. In following paragraphs, the coarse-grained ionic liquid model is combined with coarse-grained Nafion model to study

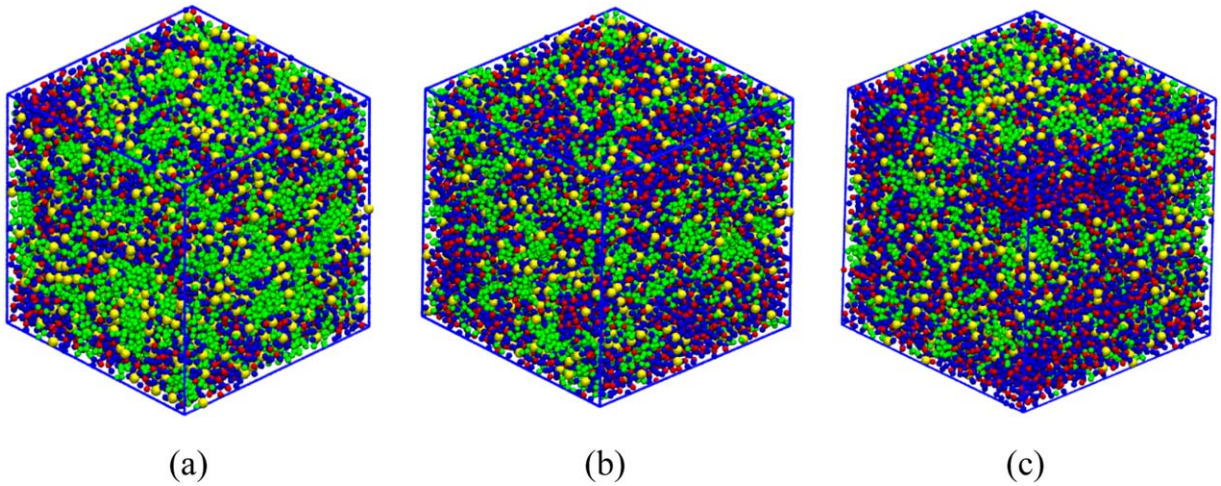

Figure 5. Ionic liquid clusters formed inside Nafion/[bmim][BF_4] composite membranes containing different weight fractions of ionic liquid 45% (a), 52% (b), and 57% (c).

Color representations: green (Nafion backbones); yellow (Nafion pendant charged groups); blue (cations); and red (anions). [Color figure can be viewed in the online issue, which is available at wileyonlinelibrary.com.]

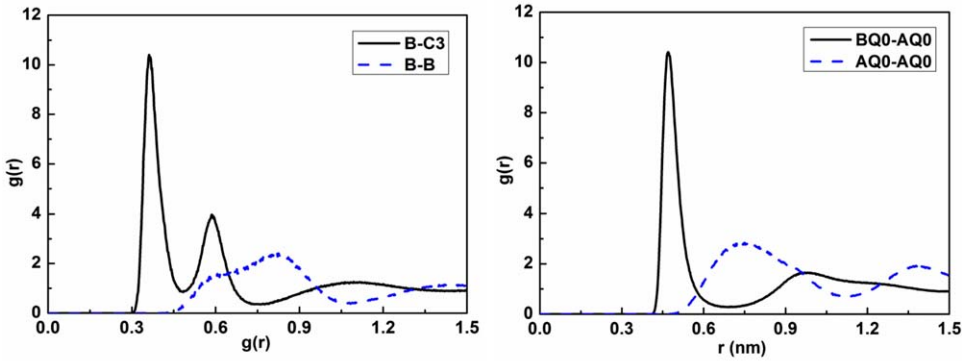

Figure 6. RDFs plotted between baron–C3 atom pairs and baron–baron atom pairs from all-atom model (a) and RDFs plotted between BQ0—AQ0 and AQ0—AQ0 bead pairs from coarse-grained model (b).

[Color figure can be viewed in the online issue, which is available at wileyonlinelibrary.com.]

structural and dynamical properties of Nafion/[bmim][BF_4] composite membrane.

Nafion-[bmim][BF_4] composite membrane

Membrane Microstructure. The microstructure of Nafion membrane is a subject of strong controversy and has attracted intensive studies. For Nafion–ionic liquid composite membranes, ionic liquid clusters have been reported to be formed inside Nafion membrane by experimental studies.[8,12,15,16] Nevertheless, molecular details regarding the composite membrane's microstructures still remain ambiguous. Figure 5a–c displays snapshots of composite membranes with varying ionic liquid concentrations after 300-ns coarse-grained MD simulations at 373 K. The coarse-grained simulation results substantiate that ionic liquid clusters can indeed form inside Nafion. In analogy to water containing Nafion membrane, ionic liquid and deprotonated sulfonate groups form continuous ionic clusters inside the membrane. The shape and size of clusters are affected by ionic liquid content in the composite membrane. Compared with the tubular shaped water channels in water-swollen Nafion,[21] ionic liquid clusters are wider. This is probably because $[bmim]^+$ cations have hydrophobic alkyl chains that can penetrate the Nafion backbone domains. The simulated microstructures of composite membrane strongly depend on distribution of ionic liquids inside Nafion. To assess the reliability of obtained microstructures from coarse-grained simulations, we compare coarse-grained and all-atom models and examine ionic liquid distribution inside Nafion by plotting RDFs. All RDFs are analyzed at 373 K and for composite membrane containing $\lambda=1.0$ concentration of ionic liquid.

RDF analysis

Interactions Between Cations–Anions and Anions–Anions. Figure 6a shows RDF curves plotted between baron–C3 atom pair and baron–baron atom pair from all-atom simulations of Nafion/ionic liquid composite membrane. Compared with RDF curves shown in Figure 3, it is found that all RDF peak heights are significantly enhanced, whereas positions of peaks are basically not altered when ionic liquids are confined in Nafion. The RDF peak enhancement phenomenon was previously reported for water molecules confined in Nafion.[43,49,50] The RDF peak height enhancement is a clear indication of heterogeneous distribution of ionic liquid clusters inside Nafion as revealed by our coarse-grained simulations. Figure 6b shows RDF curves plotted between cation–anion and anion–anion bead pairs from coarse-grained model of Nafion/ionic liquid composite membrane. Compared with Figure 1a, the coarse-grained model also reflects the RDF peak enhancement phenomenon when ionic liquids are confined in Nafion.

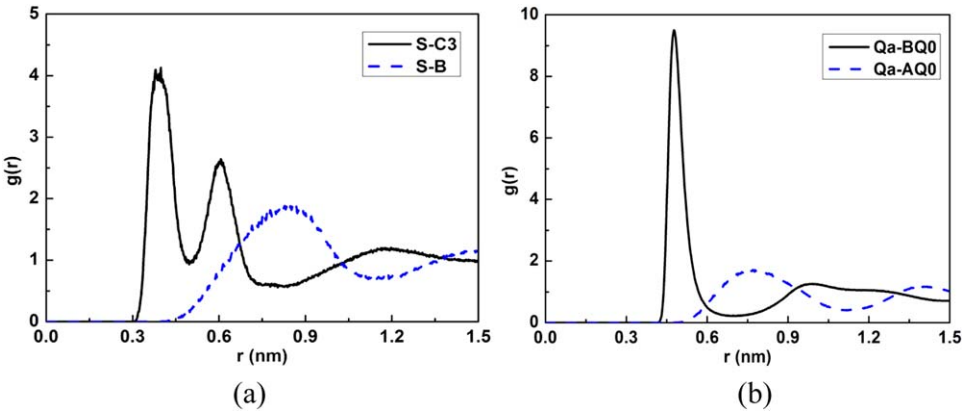

Figure 7. RDFs plotted between sulfur–C3 atom pairs and sulfur–baron atom pairs from all-atom model (a) and RDFs plotted between Qa—BQ0 and Qa—AQ0 bead pairs from coarse-grained model (b).

[Color figure can be viewed in the online issue, which is available at wileyonlinelibrary.com.]

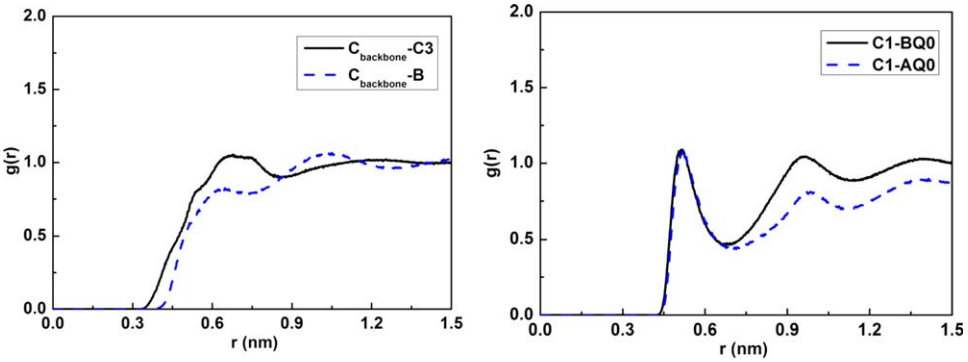

Figure 8. RDFs plotted between Nafion backbone carbon and C3 atom pairs and Nafion backbone carbon–baron atom pairs from all-atom model (a) and RDFs plotted between C1—BQ0 and C1—AQ0 bead pairs from coarse-grained model (b).

[Color figure can be viewed in the online issue, which is available at wileyonlinelibrary.com.]

Interactions Between Nafion and Ionic Liquid. Nafion is amphiphilic macromolecule consisting of hydrophobic backbones and hydrophilic pendant sulfonate groups. In this work, interactions between ionic liquid and Nafion are investigated by taking into account of both hydrophilic and hydrophobic domains of Nafion. Figure 7a shows RDF curves plotted between sulfur–C3 and sulfur–boron atom pairs. The curve shape of $g_{S-C3}(r)$ is very similar to that of $g_{B-C3}(r)$, whereas the first peak height of $g_{S-C3}(r)$ is much lower than that of $g_{B-C3}(r)$ (see Figure 6a). This phenomenon suggests that negatively charged sulfonate groups tend to attract $[bmim]^+$ cations mainly through electrostatic interactions, yet their imidazolium rings binding ability is weaker than that of BF_4^- anions. The averaged binding energy between oppositely charged species are estimated using

$$E_{binding} = \frac{E_{vdm} + E_{elec}}{N} \tag{5}$$

where E_{vdm} and E_{elec} are summed nonbonded interaction energies between sulfonate groups and $[bmim]^+$ cations or nonbonded interaction energies between BF_4^- anions and $[bmim]^+$ cations; N represents the number of sulfonate groups or BF_4^- anions in the composite membrane. The derived binding energy for (SO_3^-)–$[bmim]^+$ is -27.4 kcal mol^{-1}, and the binding energy for $[bmim]^+$–BF_4^- pair is -52.1 kcal mol^{-1}. Figure 7b is RDF curves plotted between Qa-BQ0 and Qa-AQ0 bead pairs from coarse-grained models. In the coarse-grained model, interactions between sulfonate groups and ionic liquid cations may be overestimated by the BMW-MARTINI force field, as the peak height of $g_{Qa-BQ0}(r)$ is only slightly lower than that of $g_{AQ0-BQ0}(r)$ (see Figure 6b). Nevertheless, this overestimation should have little effect on the simulated microstructures of composite membrane, as charged sulfonate groups are expected to blend with ionic liquids even interactions between sulfonate groups and cations are relatively weaker.

Figure 8a shows RDF curves plotted between Nafion backbone atoms and C3, B atoms on ionic liquid cations and anions from all-atom model. Figure 8b is corresponding RDF curves plotted between Nafion backbone beads (C1) and BQ0, AQ0 beads from coarse-grained model. Both all-atom and coarse-grained simulation results suggest that interactions between [bmim][BF_4] ionic liquid and Nafion backbone domains are very weak.

RDFs results demonstrate that the coarse-grained model can reproduce most essential structural properties of Nafion/ionic liquid composite membrane. Therefore, the simulated microstructures of composite membrane from coarse-grained models should be sound.

Confinement effect of Nafion on self-diffusion coefficients of ionic liquid

Polymer confinement effect on molecular diffusion is an interesting subject. Studying diffusion behavior of ionic liquids confined in polymers is fundamental for developing electrochemical devices such as ionogels and nanostructured proton exchange membranes. Self-diffusion coefficients of ionic liquids confined in Nafion are computed using Eq. 4, while it should be noted that usage of Einstein equation relies on the assumption that diffusing molecules have performed sufficient number of normal diffusive events through the polymer matrix. According to previous studies,[51–53] the criterion for molecules reaching normal diffusive regime is

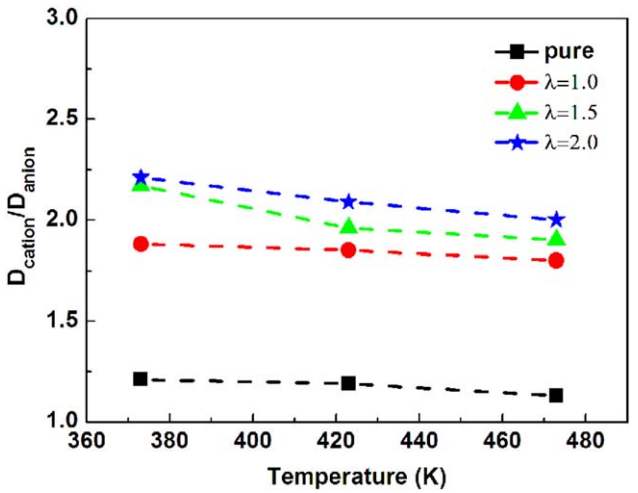

Figure 9. D_{cation}/D_{anion} ratios of pristine [bmim][BF_4] ionic liquid and [bmim][BF_4] confined in Nafion as functions of temperature and ionic liquid concentration.

[Color figure can be viewed in the online issue, which is available at wileyonlinelibrary.com.]

Table 3. Self-Diffusion Coefficients (10^{-11} m^2 s^{-1}) of [bmim][BF_4] Ionic Liquid at Different Temperatures and Different Ionic Liquid Concentrations in Nafion from All-Atom Simulations

	Cation				Anion			
Temperature (K)	Bulk	λ = 1.0	λ = 1.5	λ = 2.0	Bulk	λ = 1.0	λ = 1.5	λ = 2.0
373	2.68	0.04	0.13	0.14	2.21	0.02	0.06	0.07
423	12.91	0.67	1.07	1.26	10.80	0.36	0.54	0.60
473	31.60	3.30	4.42	8.21	27.91	1.83	2.32	4.11

Table 4. Self-Diffusion Coefficients (10^{-11} m^2 s^{-1}) of [bmim][BF_4] Ionic Liquid at Different Temperatures and Different Ionic Liquid Concentrations in Nafion from Coarse-Grained Simulations

	Cation				Anion			
Temperature (K)	Bulk	λ=1.0	λ=1.5	λ=2.0	Bulk	λ=1.0	λ=1.5	λ=2.0
373	3.50	0.67	0.83	1.11	1.61	0.31	0.38	0.49
423	9.14	4.57	5.80	6.95	5.83	2.67	3.35	4.01
473	34.40	14.63	17.89	20.39	26.57	9.86	12.56	14.28

the slope of log(MSD) vs. log t curve approaches 1. As ionic liquid's diffusion rate in Nafion is expected to be slow, long simulation time up to 100 ns is required to satisfy this requirement.

Table 3 lists calculated self-diffusion coefficients of $[bmim]^+$ cations and BF_4^- anions in the composite membrane from all-atom simulations. It can be seen that self-diffusion coefficients of bulk ionic liquids (cations and anions) are approximately 4–100 times larger than those of ionic liquids confined in Nafion depending on temperatures and ionic liquid concentrations in Nafion. Similar hindered diffusion was also found for CO_2 confined in carbon lit pores.[54] Increasing ionic liquid concentrations in Nafion or elevating temperatures in the range of 373–473 K can enhance ionic liquid's self-diffusion rate. Figure 9 plots self-diffusion coefficient ratios of cations and anions (D_{cation}/D_{anion}) as functions of temperature and ionic liquid concentration in Nafion. In all simulation models, $[bmim]^+$ cations have larger self-diffusion coefficients than BF_4^- anions while notably this phenomenon is more pronounced when ionic liquids are confined in Nafion. Analogous finding has been reported by Hou et al.[55] In their experimental study, it was found that D_{cation}/D_{anion} ratio for 1-ethyl-3-methylimidazolium tetrafluoroborate ([emim][BF_4]) ionic liquid confined in Nafion is larger than that of bulk [emim][BF_4] ionic liquid. Hoarfrost et al.[56] also reported their finding that cations diffuse faster than anions for imidazolium bis(trifluoromethane)sulfonamide ([Im][TFSI]) ionic liquid confined in poly(styrene-*b*-2-vinyl pyridine) polymers. In this study, we consider the faster diffusion of $[bmim]^+$ cations in Nafion arising from the relatively weaker binding energy between $[bmim]^+$ cations and sulfonate groups and the excessive number of $[bmim]^+$ cations in the simulation system.

The simulated self-diffusion coefficients of ionic liquid from coarse-grained models are listed in Table 4. Self-diffusion coefficients of bulk ionic liquid calculated from coarse-grained models are in satisfying agreement with results from all-atom models. While in the case of composite membrane, self-diffusion coefficients of ionic liquid calculated from coarse-grained simulations are nearly one order of magnitude larger than those calculated from all-atom simulations. This discrepancy is mainly caused by different weight fractions of ionic liquid in Nafion membrane. In all-atom models, the weight fractions of ionic liquid in the composite membrane are 24.2, 29.5, and 34.1%, respectively; while in coarse-grained models, weight fractions of ionic liquid in three composite membranes are 45, 52, and 57%. Even so, the coarse-grained models can also reflect effects of temperature and ionic liquid concentration on self-diffusion coefficients of ionic liquids confined in Nafion.

Conclusions

In this study, all-atom and coarse-grained molecular dynamics simulations are combined to understand structural and transport properties of Nafion/[bmim][BF_4] ionic liquid composite membranes. To achieve this aim, we first developed a simple yet reliable coarse-grained model for [bmim][BF_4] ionic liquid in the framework BMW-MARTINI force field. This model is proven to be able to well reproduce both structural and dynamical properties of [bmim][BF_4] ionic liquid in a wide temperature range. Nafion/[bmim][BF_4] composite membranes were then simulated using all-atom and coarse-grained simulations. Most RDF results from coarse-grained models were consistent with those from all-atom simulations, which verify the reliability of the coarse-grained model of composite membrane. Our simulations reveal that ionic liquid can indeed form clusters inside Nafion membrane substantiating experimental results. Interestingly, we found that $[bmim]^+$ cations have faster self-diffusion coefficient than BF_4^- anions while this phenomenon is more pronounced when ionic liquids are confined in Nafion. This phenomenon may be caused by the relative weaker binding energy between sulfonate groups and ionic liquid cations. The molecular understanding of Nafion/ionic liquid composite membranes could be used for the better development of elevated-temperature fuel cells.

Acknowledgments

Supports from the Program for New Century Excellent Talents in University (NCET-07-0313), National Natural Science Foundation of China (No. 20706019, 20876052), and Guangdong Science Foundation (No. S2011010002078) are gratefully acknowledged. An allocation time from the SCUTGrid at South China University of Technology and National Supercomputing Center (Shenzhen) is gratefully acknowledged.

Literature Cited

1. Zhang JL, Xie Z, Zhang JJ, Tang YH, Song CJ, Navessin T, Shi ZQ, Song DT, Wang HJ, Wilkinson DP, Liu ZS, Holdcroft S. High temperature PEM fuel cells. *J Power Sources*. 2006;160:872–891.
2. He RH, Li QF, Jensen JO, Bjerrum NJ. Doping phosphoric acid in polybenzimidazole membranes for high temperature proton exchange membrane fuel cells. *J Polym Sci Part A: Polym Chem*. 2007;45:2989–2997.
3. Li QF, Jensen JO, Savinell RF, Bjerrum NJ. High temperature proton exchange membranes based on polybenzimidazoles for fuel cells. *Prog Polym Sci*. 2009;34:449–477.
4. Feng HJ, Zhou J, Qian Y. Atomistic simulations of the solid–liquid transition of 1-ethyl-3-methyl imidazolium bromide ionic liquid. *J Chem Phys*. 2012;135:144501.
5. Shao ZG, Joghee P, Hsing IM. Preparation and characterization of hybrid Nafion-silica membrane doped with phosphotungstic acid for high temperature operation of proton exchange membrane fuel cells. *J Membr Sci*. 2004;229:43–51.
6. Hogarth WHJ, da Costa JCD, Lu GQ. Solid acid membranes for high temperature (>140°C) proton exchange membrane fuel cells. *J Power Sources*. 2005;142:223–237.
7. Di Noto V, Negro E, Sanchez JY, Lojoju C. Structure-relaxation interplay of a new nanostructured membrane based on tetraethylammonium trifluoromethanesulfonate ionic liquid and neutralized Nafion 117 for high-temperature fuel cells. *J Am Chem Soc*. 2010;132:2183–2195.
8. Mistry MK, Subianto S, Choudhury NR, Dutta NK. Interfacial interactions in aprotic ionic liquid based protonic membrane and its correlation with high temperature conductivity and thermal properties. *Langmuir*. 2009;25:9240–9251.
9. Neves LA, Coelhoso IM, Crespo JG. Methanol and gas crossover through modified Nafion membranes by incorporation of ionic liquid cations. *J Membr Sci*. 2010;360:363–370.
10. Schmidt C, Gluck T, Schmidt-Naake G. Modification of Nafion membranes by impregnation with ionic liquids. *Chem Eng Technol*. 2008;31:13–22.
11. Bennett MD, Leo DJ, Wilkes GL, Beyer FL, Pechar TW. A model of charge transport and electromechanical transduction in ionic liquid-swollen Nafion membranes. *Polymer*. 2006;47:6782–6796.
12. Mistry MK, Choudhury NR, Dutta NK, Knott R. Nanostructure evolution in high-temperature perfluorosulfonic acid ionomer membrane by small-angle X-ray scattering. *Langmuir*. 2010;26:19073–19083.
13. Schauer J, Sikora A, Pliskova M, Malis J, Mazur P, Paidar M, Bouzek K. Ion-conductive polymer membranes containing 1-butyl-3-methylimidazolium trifluoromethanesulfonate and 1-ethylimidazolium trifluoromethanesulfonate. *J Membr Sci*. 2011;367:332–339.
14. Sekhon SS, Park JS, Cho E, Yoon YG, Kim CS, Lee WY. Morphology studies of high temperature proton conducting membranes containing hydrophilic/hydrophobic ionic liquids. *Macromolecules*. 2009;42:2054–2062.
15. Sekhon SS, Park JS, Baek JS, Yim SD, Yang TH, Kim CS. Small-angle X-ray xcattering study of water free fuel cell membranes containing ionic liquids. *Chem Mater*. 2009;22:803–812.
16. Sekhon SS, Park JS, Choi YW. A SAXS study on nanostructure evolution in water free membranes containing ionic liquid: from dry membrane to saturation. *Phys Chem Chem Phys*. 2010;12:13763–13769.
17. Devanathan R, Venkatnathan A, Dupuis M. Atomistic simulation of nafion membrane. 2. dynamics of water molecules and hydronium ions. *J Phys Chem B*. 2007;111:13006–13013.
18. Jang SS, Molinero V, Cagin T, Goddard WA. Nanophase-segregation and transport in Nafion 117 from molecular dynamics simulations: effect of monomeric sequence. *J Phys Chem B*. 2004;108:3149–3157.
19. Vishnyakov A, Neimark AV. Molecular simulation study of Nafion membrane solvation in water and methanol. *J Phys Chem B*. 2000;104:4471–4478.
20. Malek K, Eikerling M, Wang QP, Liu ZS, Otsuka S, Akizuki K, Abe M. Nanophase segregation and water dynamics in hydrated Nafion: molecular modeling and experimental validation. *J Chem Phys*. 2008;129:204702.
21. Sun DL, Zhou J. Dissipative particle dynamics simulations on mesoscopic structures of Nafion and PVA/Nafion blend membranes. *Acta Phys Chim Sin*. 2012;28:909–916.
22. Wu DS, Paddison SJ, Elliott JA. A comparative study of the hydrated morphologies of perfluorosulfonic acid fuel cell membranes with mesoscopic simulations. *Energ Environ Sci*. 2008;1:284–293.
23. Yamamoto S, Hyodo SA. A computer simulation study of the mesoscopic structure of the polyelectrolyte membrane Nafion. *Polym J*. 2003;35:519–527.
24. Wu Z, Cui Q, Yethiraj A. A new coarse-grained model for water: the importance of electrostatic interactions. *J Phys Chem B*. 2010;114:10524–10529.
25. Wu Z, Cui Q, Yethiraj A. A new coarse-grained force field for membrane-peptide simulations *J Chem Theory Comput*. 2011;7:3793–3802.
26. Marrink SJ, Risselada HJ, Yefimov S, Tieleman DP, de Vries AH. The MARTINI force field: coarse grained model for biomolecular simulations. *J Phys Chem B*. 2007;111:7812–7824.
27. Lin JQ, Zheng YG, Zhang HW, Chen Z. A simulation study on nanoscale holes generated by gold nanoparticles on negative lipid bilayers. *Langmuir*. 2011;27:8323–8332.
28. Wong-Ekkabut J, Baoukina S, Triampo W, Tang IM, Tieleman DP, Monticelli L. Computer simulation study of fullerene translocation through lipid membranes. *Nat Nanotechnol*. 2008;3:363–368.
29. Patra N, Kral P. Controlled self-assembly of filled micelles on nanotubes. *J Am Chem Soc*. 2011;133:6146–6149.
30. Dong J, Zhou J. Solvent responsive block and mixed polymer brush modified amphiphilic gold nanoparticles. *Macromol Theory Simul*. 2013;doi: 10.1002/mats.201200078.
31. Liu ZP, Wu, XP, Wang, WC. A novel united-atom force field for imidazolium-based ionic liquids. *Phys Chem Chem Phys*. 2006;8:1096–1104.
32. Berendsen HJC, Postma JPM, van Gunsteren WF, DiNola A, Haak JR. Molecular dynamics with coupling to an external bath. *J Chem Phys*. 1984;81(8):3684–3690.
33. Essmann U, Perera L, Berkowitz ML, Darden T, Lee H, Pedersen LG. A smooth particle mesh Ewald method. *J Chem Phys*. 1995;103(19):8577–8593.
34. Hess B. GROMACS 4: algorithms for highly efficient, load-balanced, and scalable molecular simulation. *J Chem Theory Comput*. 2008;4:435–447.
35. Martinez JM, Martinez L. Packing optimization for automated generation of complex system's initial configurations for molecular dynamics and docking. *J Comput Chem*. 2003;24:819–825.
36. Plimpton S. Fast parallel algorithms for short-range molecular dynamics. *J Comput Phys*. 1995;117:1–19.
37. Swope WC, Andersen HC, Hans C, Berens PH, Wilson KR. A computer simulation method for the calculation of equilibrium constants for the formation of physical clusters of molecules: application to small water clusters. *J Chem Phys*. 1982;76:637–649.
38. Hoover WG. Canonical dynamics: equilibrium phase-space distributions. *Phys Rev A*. 1985;31:1695–1697.
39. Nose S. A unified formulation of the constant temperature molecular dynamics methods. *J Chem Phys*. 1984;81:511–519.
40. Andersen HC. Molecular dynamics simulations at constant pressure and/or temperature. *J Chem Phys*. 1980;72:2384–2393.
41. Liu ZP, Huang SP, Wang WC. A refined force field for molecular simulation of imidazolium-based ionic liquids. *J Phys Chem B*. 2004;108:12978–12989.
42. Wang JM, Wolf RM, Caldwell JW, Kollman PA, Case DA. Development and testing of a general amber force field. *J Comput Chem*. 2004;25:1157–1174.
43. Venkatnathan A, Devanathan R, Dupuis M. Atomistic simulations of hydrated Nafion and temperature effects on hydronium ion mobility. *J Phys Chem B*. 2007;111:7234–7244.
44. Hockney RW, Eastwood JW. Computer Simulation Using Particles. New York: McGraw-Hill International Book Co., 1981.
45. Merlet C, Salanne, M, Rotenberg, B. New coarse-grained models of imidazolium ionic liquids for bulk and interfacial molecular simulations. *J Phys Chem C*. 2012;116:7687–7693.
46. Morrow TI, Maginn EJ. Molecular structure of various ionic liquids from gas phase ab initio calculations. In: Rogers RD, Seddon KR, editors. Ionic Liquids as Green Solvents: Progress and Prospects. ACS Symposium Series, Vol. 856. 2003:162–173.
47. Kowsari MH, Alayi S, Ashrafizaadeh M, Najafi B. Molecular dynamics simulation of imidazolium-based ionic liquids. I. Dynamics and diffusion coefficient. *J Chem Phys*. 2008;129:224508.
48. Maginn EJ. Molecular simulation of ionic liquids: current status and future opportunities. *J Phys: Condens Matter*. 2009;21:373101.
49. Cui ST, Liu J, Selvan ME, Keffer DJ, Edwards BJ, Steele WV. A molecular dynamics study of a Nafion polyelectrolyte membrane and the aqueous phase structure for proton transport. *J Phys Chem B*. 2007;111:2208–2218.

50. Liu J, Suraweera N, Keffer DJ, Cui ST, Paddison SJ. On the relationship between polymer electrolyte structure and hydrated morphology of perfluorosulfonic acid membranes. *J Phys Chem C*. 2010;114:11279–11292.
51. Müller-Plathe F. Permeation of polymers—a computational approach. *Acta Polym*. 1994;45:259–293.
52. Sun DL, Zhou J. Effect of water content on microstructures and oxygen permeation in PSiMA-IPN-PMPC hydrogel: a molecular simulation study. *Chem Eng Sci*. 2012;78:236–245.
53. Sun DL, Zhou J. Molecular simulation study of oxygen sorption and diffusion in poly(lactic acid). *Chinese J Chem Eng*. 2013; doi: 10.1016/S1004-9541(13)60483-8.
54. Zhou J, Wang WC. Adsorption and diffusion of supercritical carbon dioxide in slit carbon pores. *Langmuir* 2000;16:8063–8070.
55. Hou JB, Zhang ZY, Madsen LA. Cation/anion associations in ionic liquids modulated by hydration and ionic medium. *J Phys Chem B*. 2011;115:4576–4582.
56. Hoarfrost ML, Tyagi MS, Segalman RA, Reimer JA. Effect of confinement on proton transport mechanisms in block copolymer/ionic liquid membranes. *Macromolecules*. 2012;45:3112–3320.

Manuscript received July 8, 2012, and revision received Dec. 17, 2012.